



HAL
open science

Adverse Role of Shape and Size in Second-Harmonic Scattering from Gold Nanoprisms

Krzysztof Nadolski, Emmanuel Benichou, Nina Tarnowicz-Staniak, Andrzej Żak, Christian Jonin, Katarzyna Matczyszyn, Pierre-François Brevet

► **To cite this version:**

Krzysztof Nadolski, Emmanuel Benichou, Nina Tarnowicz-Staniak, Andrzej Żak, Christian Jonin, et al.. Adverse Role of Shape and Size in Second-Harmonic Scattering from Gold Nanoprisms. *Journal of Physical Chemistry C*, 2020, 124, pp.14797 - 14803. 10.1021/acs.jpcc.0c03489 . hal-03004746

HAL Id: hal-03004746

<https://hal.science/hal-03004746>

Submitted on 13 Nov 2020

HAL is a multi-disciplinary open access archive for the deposit and dissemination of scientific research documents, whether they are published or not. The documents may come from teaching and research institutions in France or abroad, or from public or private research centers.

L'archive ouverte pluridisciplinaire **HAL**, est destinée au dépôt et à la diffusion de documents scientifiques de niveau recherche, publiés ou non, émanant des établissements d'enseignement et de recherche français ou étrangers, des laboratoires publics ou privés.

Adverse Role of Shape and Size in Second-Harmonic Scattering from Gold Nanoprisms

Krzysztof Nadolski, Emmanuel Benichou, Nina Tarnowicz-Staniak, Andrzej Żak, Christian Jonin, Katarzyna Matczyszyn,* and Pierre-François Brevet*

Cite This: *J. Phys. Chem. C* 2020, 124, 14797–14803

Read Online

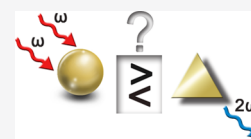
ACCESS |

Metrics & More

Article Recommendations

Supporting Information

ABSTRACT: Gold nanoparticles are widely used in different fields. They are currently under extensive investigation with regard to their linear and nonlinear optical properties. So far, nanoparticles with centrosymmetrical shapes, such as nanospheres or nanorods, have received the main attention. In this work, the properties of gold nanoprisms exhibiting a highly noncentrosymmetrical threefold symmetry are investigated with hyper-Rayleigh scattering (HRS). Aqueous solutions of gold nanospheres and nanoprisms with different sizes were synthesized. The first hyperpolarizability magnitudes of both the nanospheres and nanoprisms were determined separately with the assumption of a surface origin of the nonlinearity. Using polarization-resolved HRS, retardation is shown to be largely underdeveloped for the nanoprisms as opposed to the nanospheres. The nanoprism shape noncentrosymmetry has therefore a leading role in the HRS response although it is also shown that surface defects induce deviations from the ideal threefold symmetry.



INTRODUCTION

Metallic nano-objects, such as gold, silver, or platinum nanoparticles with a size of the order of 100 nanometers or smaller, have been gaining growing interest over the last few years driven by the potential applications envisaged. They exhibit localized surface plasmon resonances (LSPR) due to the oscillation of their conduction band electrons within a small volume yielding enhanced electromagnetic fields in their immediate vicinity providing unique optical properties.¹ LSPR can be adjusted by factors such as size, shape, material, morphology, or environments. Hence, metallic nanoparticles offer a large range of capabilities, and many applications have been proposed and realized based on these properties, from nanoantennas for sensing^{2,3} to bioimaging^{4,5} or drug delivery.⁶ Their linear optical properties based on the LSPR are now well understood and documented.^{7,8} However, this ability to enhance electromagnetic fields in a small volume has also sparked deep interest in their nonlinear optical response that can benefit as well from this feature through enhanced cross-sections.

Second-harmonic generation (SHG), the simplest of the nonlinear optical phenomena involving the conversion of two photons at a fundamental frequency into a single photon at the harmonic one, has been at the center of intense research efforts.^{9,10} At the nanoscale, where phase matching becomes irrelevant, this conversion phenomenon is extremely sensitive to the symmetry of the nano-object shape.¹¹ It is therefore crucial to perform experiments in the absence of any supporting substrates to ensure that the SHG response is solely due to the nanoparticles and is not affected by the substrate. This condition can be attained with second-harmonic scattering, also known as hyper-Rayleigh scattering

(HRS),¹² that has now become the main method for the determination of the first hyperpolarizability of molecules and nanoparticles dispersed in liquid solutions.¹³

The determination of the first hyperpolarizability of a large variety of metallic nanoparticles has already been reported. Those studies have shown that the origin of the HRS response essentially stems from the nanoparticle surface, being effectively a local electric dipole contribution at the first order owing to the centrosymmetry of the crystal lattice with weaker contributions from higher orders like field gradients. Shape is therefore critical in determining the absolute value of first hyperpolarizabilities although size must also be accounted for. Nanospheres,¹⁴ nanorods,¹⁵ or nanocubes¹⁶ have thus been extensively studied in the past few decades. In addition, deviation from the perfect geometrical shape caused by the nonideality of the nanoparticle surface due to roughness or shape defects like faceting or tip rounding is also essential in determining the HRS response.¹⁷ Nevertheless, a crucial issue that still remains is dealing with the competition between the relative influence of shape and size. Indeed, retardation, or the variation of the spatial phase of the electromagnetic fields over distances equal to the size of the nanoparticles, dramatically modifies the HRS response for gold nanoparticles having sizes larger than 50 nm and even smaller sizes for silver nanoparticles. Retardation indeed favors the electric quadru-

Received: April 20, 2020

Revised: June 9, 2020

Published: June 15, 2020



pole contribution in particular and higher multipole orders as well.^{16,18} In order to fully understand the HRS response from all these nanoparticles, many different approaches have been proposed.^{19–24} Recently, a simple model based on non-polarizable nonlinear dipoles has also been proposed to investigate this question.²⁵ In this approach, the nanoparticles are described with a small set of nonlinear dipoles. For nanocubes, this number is reduced to eight and corresponds to the eight corners acting as localized regions where the electromagnetic field enhancements are the largest.

Experiments on noncentrosymmetrical plasmonic nanoparticles have been reported for gold nanodecahedra.²⁶ Although decahedra have no symmetry center, they behave like centrosymmetrical nanoparticles due to the accidental cancellation of the response associated with a symmetry-five stemming from the two back-to-back pentagonal pyramids. In order to go further into this direction, we investigate here the case of gold nanoprisms, also known as nanotriangles or triangular nanoplates. These nanoparticles are noncentrosymmetric due to their intrinsic threefold symmetry. First hyperpolarizabilities have already been reported^{27,28} but here, we wish to discuss the signal contribution of shape non-centrosymmetry versus size retardation from an experimental point of view as this has not been performed before. In addition, the question of the presence of nanospheres in non-negligible amounts among the nanoprisms must be addressed. We therefore discuss initially the determination of the absolute first hyperpolarizabilities of both the gold nanoprisms and nanospheres. Then, polarization-resolved HRS experiments are presented to provide a quantitative analysis of the competition between the relative influence of centrosymmetry and retardation.

EXPERIMENTAL SECTION

Four different aqueous solutions of gold nanoparticles were obtained, as presented in Table 1. The edge length

Table 1. Nanoprism Solution Content, Nanoprism Average Edge Length, and Nanosphere Average Diameter in the Obtained Samples as Determined from TEM Images

sample	nanoprism content (%)	edge length (nm)	diameter (nm)
#26	42	26 ± 8	23 ± 6
#61	47	61 ± 15	44 ± 21
#78	74	78 ± 21	57 ± 22
#87	66	87 ± 21	63 ± 30

corresponds to the nanospheres, since the solutions were mixtures of nanoprisms and nanospheres. Synthesis and characterization of the nanoparticles, as well as the optical setup, are described in the Supporting Information.

RESULTS AND DISCUSSION

First Hyperpolarizability. The first hyperpolarizability values were obtained by the standard technique of HRS. It has been previously shown that plotting the HRS intensity as a function of the solution nanoparticle concentration yields a line whose slope p is related to the first hyperpolarizability as

$$p = \frac{\langle \beta_s^2 \rangle}{N_w \langle \beta_w^2 \rangle} \quad (1)$$

In eq 1, $\langle \beta_s^2 \rangle$ and $\langle \beta_w^2 \rangle$ are the squares of the first hyperpolarizabilities of the nanoparticles and the solvent molecules, here water, in the laboratory frame averaged over all orientations, and N_w is the number of solvent molecules per unit volume. The sample concentrations were determined from their gold atom content calculated from the 400 nm absorbance where surface plasmon resonances do not play any role²⁹ and the nanoparticle size obtained from the TEM pictures. The crystal structure of gold was assumed to be *fcc* with a unit cell size of 0.408 nm.³⁰ The first hyperpolarizability value of water was taken as 0.087×10^{-30} esu and used as the internal reference as reported by Duboisset et al.³¹

The plots of the HRS intensity as a function of the nanoparticle concentration normalized to the neat solvent intensity are presented in Figure 1a,b. Since sample #26 was

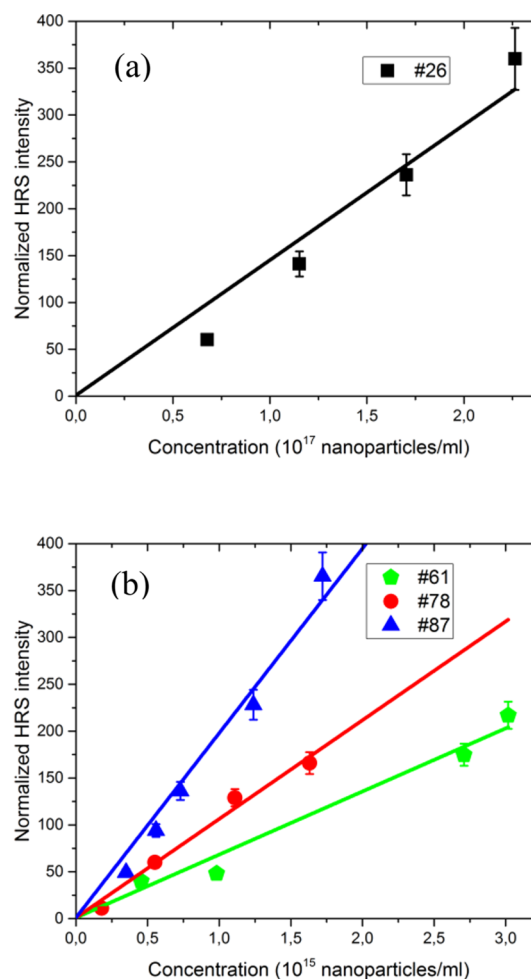


Figure 1. Solvent normalized HRS intensity for samples (a) #26, (b) #61, #78, and #87 as a function of the nanoparticle concentration. Solid lines are the corresponding linear fits with the intercept set to unity.

obtained by a separate synthesis protocol, its initial nanoparticle concentration is notably higher and is therefore presented on a separate graph for improved clarity. Uncertainties were calculated by applying simple counting statistics methods. The first hyperpolarizability values as given by eq 1 and reported in Table 2 where β stands for $\sqrt{\langle \beta_s^2 \rangle}$ must be attributed to the mixture of nanoprisms and nanospheres. Because the HRS intensity is additive, we have

$$\langle \beta_s^2 \rangle = \alpha \langle \beta_{\text{nP}}^2 \rangle + (1 - \alpha) \langle \beta_{\text{nS}}^2 \rangle \quad (2)$$

Table 2. First Hyperpolarizability β and First Hyperpolarizability per Unit Surface β_0 for the Nanospheres in all Samples

sample	β (esu)	β_0 (esu/nm ²)
#26	0.5×10^{-27}	3.3×10^{-31}
#61	4.0×10^{-27}	6.6×10^{-31}
#78	5.0×10^{-27}	4.9×10^{-31}
#87	6.8×10^{-27}	5.4×10^{-31}

by introducing the first hyperpolarizability of nanoprisms $\langle \beta_{\text{nP}}^2 \rangle$ and nanospheres $\langle \beta_{\text{nS}}^2 \rangle$. In eq 2, α is the solution content in nanoprisms as given in Table 1. The independent determination of the first hyperpolarizability of the nanoprisms and nanospheres however requires a complementary assumption.

The latter can be based on the surface origin of the first hyperpolarizability of gold nanoparticles in the size range used here where retardation is weak. In this size range, the first hyperpolarizability has been shown to scale with the surface area of the nanoparticles.^{18,24} Therefore, if we apply this principle in the present case, with symmetry cancellation of the opposing top and bottom surface for the nanoprisms, we get

$$\sqrt{\langle \beta_{\text{nP}}^2 \rangle} = \varepsilon \sqrt{\langle \beta_{\text{nS}}^2 \rangle} \quad (3)$$

where the parameter $\varepsilon = \varepsilon_{\text{nS}}/\varepsilon_{\text{nP}}$ is the ratio of the HRS active surface area for the nanoprisms and nanospheres formally introduced through

$$\sqrt{\langle \beta_I^2 \rangle} = \int \beta_0 dA_I = \beta_0 \int dA_I = \varepsilon_I \beta_0 \quad (4)$$

where the subscript I stands for nS or nP. The integral is performed over the closed surface of the nanosphere or nanoprism, whereas β_0 stands for hyperpolarizability per unit surface. In eq 4, cancellation of terms in the integral occurs due to symmetry. Therefore, ε_I may not be equal to the geometrical surface.

Using eqs 2 and 3, we can provide the first hyperpolarizability of the nanoprisms and nanospheres for all samples, see Tables 2 and 3.

Table 3. First Hyperpolarizability β and First Hyperpolarizability per Unit Surface β_0 for the Nanoprisms in all Samples

sample	β (esu)	β_0 (esu/nm ²)
#26	0.4×10^{-27}	2.7×10^{-31}
#61	3.8×10^{-27}	4.4×10^{-31}
#78	4.7×10^{-27}	3.3×10^{-31}
#87	6.5×10^{-27}	3.6×10^{-31}

From a general standpoint, the first hyperpolarizability magnitudes determined for the gold nanospheres contained in the aqueous solution samples are much smaller than what can be obtained from the citrate reduction of the metallic salt. This feature further demonstrates the extreme sensitivity of the nanoparticle surface to the synthesis and therefore exact composition and morphology. Indeed, El Harfouch et al.¹⁵ reported first hyperpolarizability values for gold nanospheres and nanorods in the range of 10^{-25} – 10^{-24} esu, about 2 orders

of magnitude higher than those for the present gold nanoprisms, in line with data obtained for other plasmonic nanoparticles.^{16,32}

In order to further support the surface origin of the nonlinearity, the first hyperpolarizabilities were normalized per unit surface area, see Table 2. The value of about $(5 \pm 2) \times 10^{-31}$ esu/nm² is obtained. This value is constant once normalized to the nanoparticle surface area, as expected. Of note, a slightly weaker value is obtained for sample #26, possibly due to the nonresonant character of the conditions. A tentative normalization by the nanoparticle volume, data not shown, identical to a normalization by the number of atoms present in the nanoparticles, does not lead to a constant normalized first hyperpolarizability, demonstrating the effectiveness of the surface origin of the nonlinearity.

A similar analysis was then performed for the nanoprisms, and the data are reported in Table 3. The first hyperpolarizability per unit surface area for the nanoprisms is found to be $(3 \pm 2) \times 10^{-31}$ esu/nm² and, as expected, similar to that of the nanospheres, since the synthesis is identical. Considering the UV–vis absorption spectra, a non-negligible contribution from the surface plasmon resonance at a fundamental wavelength of 800 nm may be present. This is perhaps the reason for the weaker value observed for sample #26 that is off resonance at both the fundamental and the harmonic wavelengths.

Polarization Analysis. As it has been demonstrated in the past,^{15,16} increasing the size of centrosymmetrical plasmonic nanoparticles introduces a significant contribution of retardation in the total signal, observable in the polarization analysis of the HRS intensity. In this case, a clear quadrupole contribution is observed through the appearance of four lobes on the vertically polarized HRS intensity as a function of the input polarization angle. Since gold nanoprisms are noncentrosymmetrical owing to their threefold symmetry, their response is expected to noticeably deviate from this behavior. To perform this polarization-resolved study, an analyzer was placed before the spectrometer. The polar plot of sample #26 is presented in Figure 2, and the polar plots for the other samples are provided in the Supporting Information. They are all very similar irrespective of the nanoprism edge length.

All obtained polar graphs were then adjusted with the following expression³³ following the standard procedure:

$$I^X = a^X \cos^4 \gamma + b^X \cos^2 \gamma \sin^2 \gamma + c^X \sin^4 \gamma \quad (5)$$

where X corresponds to the vertical V or horizontal H output polarization selection, and a^X , b^X , and c^X are three intensity parameters, whereas γ is the input fundamental polarization angle. From these parameters and following previous works, three parameters were determined from eq 5. The first one is known as the depolarization ratio defined as

$$D^V = c^V/a^V \quad (6)$$

The two other parameters are termed the retardation parameters for the V and H polarized intensity and are defined as^{15,34}

$$\zeta^V = (b^V - a^V - c^V)/b^V \quad (7)$$

$$\zeta^H = (a^H - c^H)/(a^H + c^H) \quad (8)$$

The experimentally determined depolarization and retardation parameters are presented in Table 4. Both parameters ζ^V

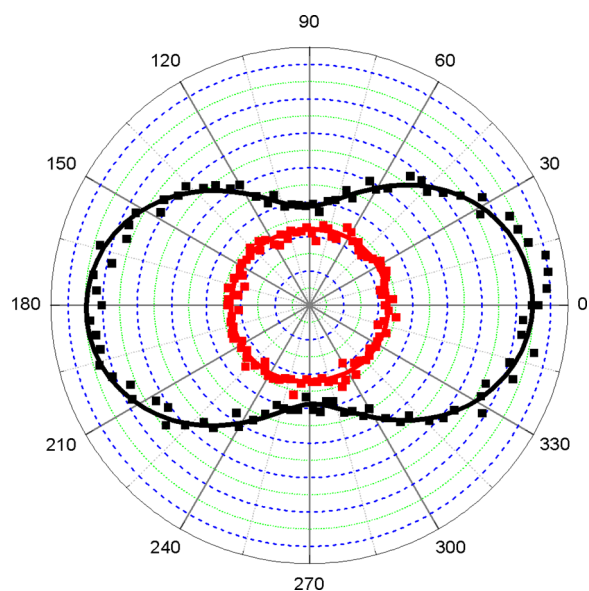


Figure 2. Polar plots of sample #26. The black curve represents vertically polarized HRS intensity, and the red curve represents horizontally polarized HRS intensity.

Table 4. Retardation Parameters ζ^V and ζ^H and Depolarization Ratio D^V for All Samples

sample	ζ^V	ζ^H	D^V
#26	0.04	0.02	0.44
#61	0.05	0.04	0.47
#78	0.11	0.10	0.42
#87	0.09	0.10	0.42

and ζ^H grow with the nanoparticle size as expected for retardation with somewhat saturation for samples #78 and #87. However, the discussion of the size evolution of these two parameters must be performed in light of the significant nanosphere content in the samples. Indeed, this increase can be attributed to the nanospheres, as it is known that these two parameters increase with their diameter. Introducing the nanoprism content of the nanoparticle solutions, eq 5 yields

$$\zeta^X = \alpha \zeta_{\text{NP}}^X + (1 - \alpha) \zeta_{\text{NS}}^X \quad (9)$$

In principle, for perfect nanospheres, it has been shown previously that $\zeta_{\text{NS}}^V = 1$ and $\zeta_{\text{NS}}^H = 0$, namely; they exhibit a pure quadrupole response. However, in most cases, nanospheres are not perfect geometrical spheres, and shape defects induce a much reduced ζ_{NS}^V value, whereas ζ_{NS}^H remains close to zero. Because these retardation parameters do not depend on the first hyperpolarizability itself as they are effectively intensity ratios, previously reported retardation parameters can be used. Values between 0 and 0.2 have been reported for the ζ_{NS}^V retardation parameter for gold nanospheres.¹⁶ With the nanoprism contents given in Table 1, it appears that ζ_{NP}^V and ζ_{NP}^H values must vanish altogether within experimental error. Hence, despite a non-negligible size and therefore non-negligible spatial extension, nanoprisms do not exhibit significant retardation. This property results from the threefold noncentrosymmetry of their shape as opposed to the centrosymmetric nanospheres.

We now turn to the depolarization ratio D^V . A theoretical value $D^V = 0.67$ is expected for a pointlike planar threefold geometry. An archetypal system with this geometry is

represented by crystal violet. On the opposite, a value $D^V = 0.2$ is expected for a pointlike onefold system.^{35,36} The samples investigated in this study contained a significant amount of nanospheres that alters to a notable extent the assignment of this parameter to the nanoprisms only. In addition, nanoprisms are not pointlike structures. Nevertheless, the measured depolarization ratios all have values around 0.45, see Table 4, weaker than the 2/3 expected for the pure threefold symmetry but significantly different from the onefold 0.2 value. This value emphasizes the nature of the nanoparticle HRS response that arises from a spatially distributed nonlinearity. Hence, since nanospheres possess a depolarization ratio of this magnitude,³⁷ nanoprisms also exhibit depolarization ratios of 0.45. This value differs significantly from the perfect planar threefold symmetry, indicating that the nanoprism nonlinearity cannot be fully associated with such a perfect geometry. Shape defects like morphologically induced differences in the local field enhancements at the tips of the prism nanostructure must play some role.

Theoretical Simulations. In order to provide a deeper understanding of the experimental data and to unravel the origin of the HRS signals from nanoprisms, theoretical simulations were performed using a discrete nonpolarizable nonlinear dipole model.³⁸ A D_{3h} symmetry for equilateral triangles with a defined edge length was assumed, see Figure 3.

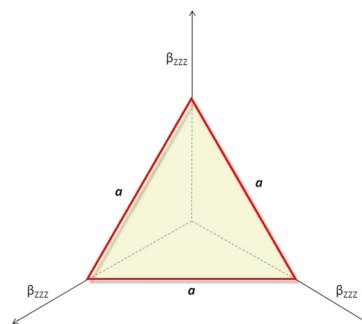


Figure 3. Schematics of the nanoprism D_{3h} symmetry assumed in the theoretical simulations.

It is interesting to note that in the case of equilateral prisms, a nonlinear response stemming from the edge surface area behaves similarly to the one arising from the three sharp tips of the nanostructure. Following the previous work reported for nanocubes, the nanoprism HRS response was assumed to stem from these three sharp tips of the structure, to which a single hyperpolarizability component β_{zzz} nonlinear dipole was attributed. Tips are known to provide large electromagnetic field enhancements and therefore are the siege of enhanced HRS. The absence of contribution from the top and bottom faces is therefore in line with the above postulated assumptions.

Using this arrangement of the three equal nonlinear dipoles, the depolarization ratio D^V , along with the two retardation parameters ζ^V and ζ^H , was simulated with respect to the nanoprism edge length, see Figure 4. The corresponding polarization-resolved HRS intensity plots for small (vanishing edge length, i.e., the three nonlinear dipoles are co-located) gold nanoprisms are given in Figure 5, meanwhile plots for large (100 nm edge length) gold nanoprisms are included in the Supporting Information. For small nanoprisms, we do not observe any retardation as expected, and the response is similar

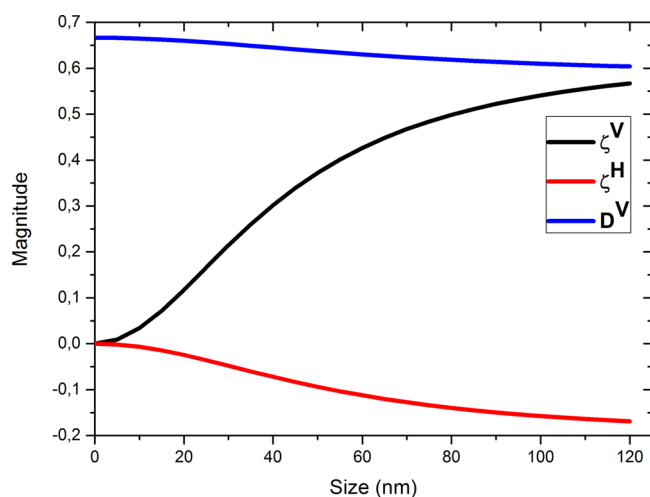


Figure 4. Simulated retardation ζ_{np}^V and ζ_{np}^H and the depolarization ratio D^V as a function of the gold nanoprism edge length.

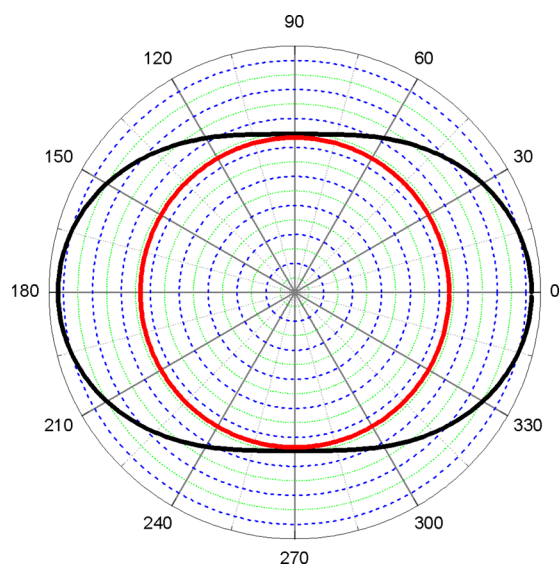


Figure 5. Polar plots for vanishingly small edge length nanoprisms. The black curve represents vertically polarized HRS intensity, and the red curve represents horizontally polarized HRS intensity.

to that of molecules with the same symmetry like crystal violet.³⁶ The polar plot of small edge length nanoprisms corresponds well to the experimentally obtained graph for sample #26, see Figure 2, i.e., showing a very low level of retardation. On the opposite, for large nanoprisms, retardation is significant. Theoretically calculated retardation parameters for the large 100 nm edge length nanoprisms are respectively $\zeta_{\text{np}}^V = 0.54$ and $\zeta_{\text{np}}^H = -0.16$, whereas the depolarization ratio has only weakly evolved from $D^V = 2/3$, its value for vanishing edge length, to $D^V = 0.61$.

Theoretical simulations provide a deeper insight into the experimental data. A similar approach was performed for silver nanocubes, as reported by Russier-Antoine et al.,¹⁶ where the simulated graphs exhibited significantly higher retardation due to the centrosymmetry of the nanocubes. For the nanoprisms, the simulations performed assuming a perfect threefold symmetry yield rather high values of the parameter ζ^V as compared to the experimental data. Introducing three unbalanced nonlinear dipoles disposed at the three tips of

the nanoprisms provides lower ζ^V values, in agreement with the experimental observations. This breaking of the perfect threefold symmetry is also seen through the depolarization ratio measured, which is weaker than the theoretical one.

CONCLUSIONS

Aqueous suspensions of gold nanoprisms with an average edge length ranging from 26 to 87 nm were successfully synthesized combining various synthesis protocols known in the literature and investigated with polarization-resolved HRS. The determined first hyperpolarizabilities are rather low as compared to the values reported in the literature for other plasmonic nanoparticle shapes, such as rods or spheres. This feature emphasizes the sensitivity of this parameter to the nature of the nanoparticle surface and must be taken into account when selecting nanostructures with an efficient HRS response. The polarization analysis supports an origin of the response stemming from the nanoparticle surface, without significant retardation contributions, although this property can also be understood similarly as stemming from the three nanoprism tips. The depolarization ratio complements this analysis and underlines the potential deviation of the nanoprism exact shape from that of perfect equilateral prisms. All these results can be rationalized with a simple model involving three nonlinear dipoles simulating the three sharp tips of the nanoprisms. Finally, it is interesting to note that this in-depth analysis of the nanoprisms is performed in the presence of nanospheres produced during the same synthesis providing evidence for information extraction from nanoparticle mixtures.

Surprisingly, the noncentrosymmetrical shape of the nanoprisms may be a disadvantage for applications like sensing, since the first hyperpolarizabilities are not as high as expected considering their noncentrosymmetric shape. This feature may result in a lower sensitivity required to probe external medium changes. This may remain to be confirmed, though the three tips may be sufficiently sensitive. In any case, the weak contribution of retardation may be profitably used, especially for the largest nanoparticles, where the first hyperpolarizability will only stem from the surface without significant contribution from the volume, a clear asset in sensing for example.

ASSOCIATED CONTENT

Supporting Information

The Supporting Information is available free of charge at <https://pubs.acs.org/doi/10.1021/acs.jpcc.0c03489>.

Detailed synthesis description, sample characterization methods, and a supplemental polar graph of theoretically simulated polarization-resolved HRS signal of big (100 nm edge length) gold nanoprisms followed by experimentally obtained polar plots of samples #61, #78, and #87 (PDF)

AUTHOR INFORMATION

Corresponding Authors

Katarzyna Matczyszyn – *Advanced Materials Engineering and Modelling Group, Wrocław University of Science and Technology, Wrocław, Poland*; orcid.org/0000-0001-8578-8340; Email: katarzyna.matczyszyn@pwr.edu.pl

Pierre-François Brevet – *Institut Lumière Matière, University of Lyon, UMR 5306 CNRS and Université Claude Bernard*

Lyon 1, Villeurbanne, France; orcid.org/0000-0002-9097-0187; Email: pfbrevet@univ-lyon1.fr

Authors

Krzysztof Nadolski – Institut Lumière Matière, University of Lyon, UMR 5306 CNRS and Université Claude Bernard Lyon 1, Villeurbanne, France; Advanced Materials Engineering and Modelling Group, Wrocław University of Science and Technology, Wrocław, Poland

Emmanuel Benichou – Institut Lumière Matière, University of Lyon, UMR 5306 CNRS and Université Claude Bernard Lyon 1, Villeurbanne, France; orcid.org/0000-0003-0590-6998

Nina Tarnowicz-Staniak – Advanced Materials Engineering and Modelling Group, Wrocław University of Science and Technology, Wrocław, Poland

Andrzej Żak – Electron Microscopy Laboratory, Faculty of Mechanical Engineering, Wrocław University of Science and Technology, Wrocław, Poland

Christian Jonin – Institut Lumière Matière, University of Lyon, UMR 5306 CNRS and Université Claude Bernard Lyon 1, Villeurbanne, France

Complete contact information is available at: <https://pubs.acs.org/10.1021/acs.jpcc.0c03489>

Author Contributions

K.M. and P.F.B. conceived and coordinated the project. K.N., E.B., and C.J. conducted the measurements. N.T.-S. synthesized the nanoparticles. N.T.-S. and A.Ż. characterized the samples. P.F.B. performed the simulations. K.N. and P.F.B. took the lead in writing the manuscript. All authors provided critical feedback and helped to shape the research, analysis, and manuscript.

Notes

The authors declare no competing financial interest.

ACKNOWLEDGMENTS

E.B., C.J., and P.F.B. thank the French Agence nationale pour la Recherche (ANR) for funding under contract number CE24-2017-RACINE. K.M., K.N., and N.T.-S. acknowledge funding from the Polish National Science Centre for support under Harmonia project UMO-2016/22/M/ST4/00275. K.M., P.F.B., K.N., N.T.-S., and C.J. thank Campus France and The Polish National Agency for Academic Exchange for financial support under PHC Polonium “NanoSHG” project PPN/BFR/2019/1/00030. K.N. thanks GDR Or-nano for a subvention for academic stay at ILM, Lyon, France. A.Ż. gratefully acknowledges funding from the National Science Centre (PL) under “Miniatura” grant number 2019/03/X/NZ3/02100. The authors thank Ms. Marta Piksa for assistance regarding the visual part of this work.

REFERENCES

- (1) Louis, C.; Pluchery, O., *Gold Nanoparticles for Physics, Chemistry, and Biology*. Imperial College Press: 2012, DOI: [10.1142/p815](https://doi.org/10.1142/p815).
- (2) Saha, K.; Agasti, S. S.; Kim, C.; Li, X.; Rotello, V. M. Gold nanoparticles in chemical and biological sensing. *Chem. Rev.* **2012**, *112*, 2739–2779.
- (3) Stipe, B. C.; Strand, T. C.; Poon, C. C.; Balamane, H.; Boone, T. D.; Katine, J. A.; Li, J.-L.; Rawat, V.; Nemoto, H.; Hirotsune, A.; et al. Magnetic recording at 1.5 Pb m⁻² using an integrated plasmonic antenna. *Nat. Photonics.* **2010**, *4*, 484–488.

- (4) Brach, K.; Olesiak-Banska, J.; Waszkielewicz, M.; Samoc, M.; Matczyszyn, K. DNA liquid crystals doped with AuAg nanoclusters: One-photon and two-photon imaging. *J. Mol. Liq.* **2018**, *259*, 82–87.
- (5) Olesiak-Banska, J.; Gordel, M.; Matczyszyn, K.; Shynkar, V.; Zyss, J.; Samoc, M. Gold nanorods as multifunctional probes in a liquid crystalline DNA matrix. *Nanoscale.* **2013**, *5*, 10975–10981.
- (6) Visaria, R. K.; Griffin, R. J.; Williams, B. W.; Ebbini, E. S.; Paciotti, G. F.; Song, C. W.; Bischof, J. C. Enhancement of tumor thermal therapy using gold nanoparticle-assisted tumor necrosis factor- α delivery. *Mol. Cancer. Ther.* **2006**, *5*, 1014–1020.
- (7) Amendola, V.; Pilot, R.; Frasconi, M.; Marago, O. M.; Iati, M. A. Surface plasmon resonance in gold nanoparticles: a review. *J. Phys. Condens. Matter.* **2017**, *29*, 203002.
- (8) Garcia, M. A. Surface plasmons in metallic nanoparticles: fundamentals and applications. *J. Phys. D: Appl. Phys.* **2011**, *44*, 283001.
- (9) Butet, J.; Brevet, P.-F.; Martin, O. J. F. Optical Second Harmonic Generation in Plasmonic Nanostructures: From Fundamental Principles to Advanced Applications. *ACS. Nano.* **2015**, *9*, 10545–10562.
- (10) Deska, R.; Olesiak-Banska, J.; Glowacki, E.; Samoc, M.; Matczyszyn, K. Two-photon excited luminescence and second-harmonic generation in quinacridone microstructures. *Dyes. Pigm.* **2020**, *177*, 108628.
- (11) Boyd, G. T.; Rasing, T.; Leite, J. R. R.; Shen, Y. R. Local-field enhancement on rough surfaces of metals, semimetals, and semiconductors with the use of optical second-harmonic generation. *Phys. Rev. B.* **1984**, *30*, 519–526.
- (12) Maker, P. D.; Terhune, R. W.; Nisenoff, M.; Savage, C. M. Effects of Dispersion and Focusing on the Production of Optical Harmonics. *Phys. Rev. Lett.* **1962**, *8*, 21–22.
- (13) Clays, K.; Persoons, A. Hyper-Rayleigh Scattering in Solution. *Phys. Rev. Lett.* **1991**, *66*, 2980–2983.
- (14) Hao, E. C.; Schatz, G. C.; Johnson, R. C.; Hupp, J. T. Hyper-Rayleigh scattering from silver nanoparticles. *J. Chem. Phys.* **2002**, *117*, 5963–5966.
- (15) El Harfouch, Y.; Benichou, E.; Bertorelle, F.; Russier-Antoine, I.; Jonin, C.; Lascoux, N.; Brevet, P.-F. Hyper-Rayleigh Scattering from Gold Nanorods. *J. Phys. Chem. C.* **2014**, *118*, 609–616.
- (16) Russier-Antoine, I.; Lee, H. J.; Wark, A. W.; Butet, J.; Benichou, E.; Jonin, C.; Martin, O. J. F.; Brevet, P.-F. Second Harmonic Scattering from Silver Nanocubes. *J. Phys. Chem. C.* **2018**, *122*, 17447–17455.
- (17) Russier-Antoine, I.; McLintock, A.; Wark, A. W.; Bertorelle, F.; Benichou, E.; Bergman, E.; Bruyere, A.; Jonin, C.; Brevet, P.-F. Hyper-Rayleigh Scattering from Gold Nanorods: The Shape Effect for Centrosymmetric Nanoparticles. *J. Phys. Chem. C.* **2014**, *8984*, 609–616.
- (18) Russier-Antoine, I.; Benichou, E.; Bachelier, G.; Jonin, C.; Brevet, P.-F. Multipolar Contributions of the Second Harmonic Generation from Silver and Gold Nanoparticles. *J. Phys. Chem. C.* **2007**, *111*, 9044–9048.
- (19) Agarwal, G. S.; Jha, S. S. Theory of second harmonic generation at a metal surface with surface plasmon excitation. *Solid. State. Commun.* **1982**, *41*, 499–501.
- (20) Hua, X. M.; Gersten, J. I. Theory of second-harmonic generation by small metal spheres. *Phys. Rev. B.* **1986**, *33*, 3756–3764.
- (21) Östling, D.; Stampfli, P.; Bennemann, K. H. Theory of nonlinear optical properties of small metallic spheres. *J. Phys. D. Atom. Mol. Clusters.* **1993**, *28*, 169–175.
- (22) Martorell, J.; Vilaseca, R.; Corbalán, R. Second harmonic generation in a photonic crystal. *Appl. Phys. Lett.* **1997**, *70*, 702–704.
- (23) Dadap, J. I.; Shan, J.; Eisenthal, K. B.; Heinz, T. F. Second-Harmonic Rayleigh Scattering from a Sphere of Centrosymmetric Material. *Phys. Rev. Lett.* **1999**, *83*, 4045–4048.
- (24) Bachelier, G.; Russier-Antoine, I.; Benichou, E.; Jonin, C.; Brevet, P.-F. Multipolar second-harmonic generation in noble metal nanoparticles. *J. Opt. Soc. Am. B.* **2008**, *25*, 955–960.

(25) Duboisset, J.; Brevet, P.-F. Second Harmonic Scattering Defined Topological Classes for Nano-Objects. *J. Phys. Chem. C* **2019**, *123*, 25303–25308.

(26) Russier-Antoine, I.; Duboisset, J.; Bachelier, G.; Benichou, E.; Jonin, C.; Del Fatti, N.; Vallee, F.; Sanchez-Inglesias, A.; Pastoriza-Santos, I.; Liz-Marzan, L. M.; Brevert, P. F.; et al. Symmetry Cancellations in the Quadratic Hyperpolarizability of Non-Centrosymmetric Gold Decahedra. *J. Phys. Chem. Lett.* **2010**, *1*, 874–880.

(27) Singh, A. K.; Senapati, D.; Neely, A.; Kolawole, G.; Hawker, C.; Ray, P. C. Nonlinear optical properties of triangular silver nanomaterials. *Chem. Phys. Lett.* **2009**, *481*, 94–98.

(28) Jain, B.; Srivastava, A. K.; Uppal, A.; Gupta, P. K.; Das, K. NIR Femtosecond Laser Induced Hyper-Rayleigh Scattering and Luminescence from Silver Nanoprisms. *J. Nanosci. Nanotechnol.* **2010**, *10*, 5826–5830.

(29) Hendel, T.; Wuithschick, M.; Kettemann, F.; Birnbaum, A.; Rademann, K.; Polte, J. In Situ Determination of Colloidal Gold Concentrations with UV-Vis Spectroscopy: Limitation and Perspectives. *Anal. Chem.* **2014**, *86*, 11115–11124.

(30) Olesiak-Banska, J.; Gordel, M.; Kolkowski, R.; Matczyszyn, K.; Samoc, M. Third-Order Nonlinear Optical Properties of Colloidal Gold Nanorods. *J. Phys. Chem. C* **2012**, *116*, 13731–13737.

(31) Duboisset, J.; Matar, G.; Russier-Antoine, I.; Benichou, E.; Bachelier, G.; Jonin, C.; Ficheux, D.; Besson, F.; Brevet, P.-F. First Hyperpolarizability of the Natural Aromatic Amino Acids Tryptophan, Tyrosine, and Phenylalanine and the Tripeptide Lysine-Tryptophan-Lysine Determined by Hyper-Rayleigh Scattering. *J. Phys. Chem. B* **2010**, *114*, 13861–13865.

(32) Minh Ngo, H.; Diep Lai, N.; Ledoux-Rak, I. High second-order nonlinear response of platinum nanoflowers: the role of surface corrugation. *Nanoscale* **2016**, *8*, 3489–3495.

(33) Nappa, J.; Revillod, G.; Russier-Antoine, I.; Benichou, E.; Jonin, C.; Brevet, P.-F. Electric dipole origin of the second harmonic generation of small metallic particles. *Phys. Rev. B* **2005**, *71*, 165407.

(34) Butet, J.; Bachelier, G.; Russier-Antoine, I.; Jonin, C.; Benichou, E.; Brevet, P.-F. Interference between Selected Dipoles and Octupoles in the Optical Second-Harmonic Generation from Spherical Gold Nanoparticles. *Phys. Rev. Lett.* **2010**, *105*, 077401.

(35) Revillod, G.; Russier-Antoine, I.; Benichou, E.; Jonin, C.; Brevet, P.-F. Investigating the Interaction of Crystal Violet Probe Molecules on Sodium Dodecyl Sulfate Micelles with Hyper-Rayleigh Scattering. *J. Phys. Chem. B* **2005**, *109*, 5383–5387.

(36) Brasselet, S.; Zyss, J. Multipolar molecules and multipolar fields: probing and controlling the tensorial nature of nonlinear molecular media. *J. Opt. Soc. Am. B* **1998**, *15*, 257–288.

(37) Nappa, J.; Russier-Antoine, I.; Benichou, E.; Jonin, C.; Brevet, P.-F. Second harmonic generation from small gold metallic particles: From the dipolar to the quadrupolar response. *J. Chem. Phys.* **2006**, *125*, 184712.

(38) Balla, N. K.; Yew, E. Y. S.; Sheppard, C. J. R.; So, P. T. C. Coupled and uncoupled dipole models of nonlinear scattering. *Opt. Express* **2012**, *20*, 25834–25842.